

Research Article: New Research | Cognition and Behavior

Oscillatory neural correlates of police firearms decision making in virtual reality

<https://doi.org/10.1523/ENEURO.0112-24.2024>

Received: 14 March 2024

Accepted: 23 May 2024

Copyright © 2024 Alexander et al.

This is an open-access article distributed under the terms of the [Creative Commons Attribution 4.0 International license](#), which permits unrestricted use, distribution and reproduction in any medium provided that the original work is properly attributed.

This Early Release article has been peer reviewed and accepted, but has not been through the composition and copyediting processes. The final version may differ slightly in style or formatting and will contain links to any extended data.

Alerts: Sign up at www.eneuro.org/alerts to receive customized email alerts when the fully formatted version of this article is published.

Oscillatory neural correlates of police firearms decision making in virtual reality

Nicholas A. Alexander^{*1,2}, Clíona L. Kelly³, Hongfang Wang⁵, Robert A. Nash², Shaun Beebe⁴, Matthew J. Brookes^{4†}, Klaus Kessler^{*2,5}

¹Wellcome Centre for Human Neuroimaging, Department of Imaging Neuroscience, UCL Queen Square Institute of Neurology, University College London, London, WC1N 3AR, UK, ²Aston Institute of Health and Neurodevelopment, College of Health and Life Sciences, Aston University, Birmingham, B4 7E, UK, ³Yale Child Study Center, Yale University School of Medicine, New Haven, Connecticut, 06520, USA, ⁴Sir Peter Mansfield Imaging Centre, School of Physics and Astronomy, University of Nottingham, Nottingham, NG7 2QX, UK, ⁵School of Psychology, University College Dublin, Dublin, D4, Ireland, [†]M.J.B. is a director of Cerca Magnetics Limited, a spin-out company whose aim is to commercialise aspects of OPM-MEG technology. M.J.B. holds founding equity in Cerca Magnetics Limited.

*Corresponding authors

Nicholas A. Alexander (n.alexander@ucl.ac.uk)
Klaus Kessler (klaus.kessler1@ucd.ie)

Abbreviated title

Neural correlates of police decision making

Acknowledgements

The authors would like to thank the Durham Constabulary and Cleveland Police for their generous support of this research project from inception and throughout. Without their guidance regarding AFO practices and provision of facilities, this project would not have been possible. We would also like to thank our colleagues at the Wellcome Centre for Human Neuroimaging, Aston Institute of Health and Neurodevelopment, and Sir Peter Mansfield Imaging Centre for valuable discussions about data analysis. We thank Nafeesa Gul for help with data collection conducted at Aston University.

Conflict of Interest

Authors report no conflict of interest

Funding sources

This project was funded through a collaboration between Aston University (50th Anniversary PhD studentship) and the University of Nottingham.

34 **Author Contributions**

35 NAA, RAN, SB, MJB and KK Designed Research; NAA, CLK and HW Performed Research;
36 NAA and HW Contributed unpublished reagents/ analytic tools; NAA, CLK, HW and MJB
37 Analyzed data; NAA, KK Wrote the paper

eNeuro Accepted Manuscript

38 **Abstract**

39 We investigated the neural signatures of expert decision making in the context of police
40 training in a virtual reality-based shoot/don't shoot scenario. Police officers can use stopping
41 force against a perpetrator, which may require using a firearm and each decision made by an
42 officer to discharge their firearm or not has substantial implications. Therefore it is important
43 to understand the cognitive and underlying neurophysiological processes that lead to such a
44 decision. We used virtual reality-based simulations to elicit ecologically valid behaviour from
45 Authorised Firearms Officers (AFOs) in the UK and matched novices in a Shoot/Don't Shoot
46 task and recorded electroencephalography concurrently. We found that AFOs had
47 consistently faster response times than novices, suggesting our task was sensitive to their
48 expertise. To investigate differences in decision making processes under varying levels of
49 threat and expertise, we analysed electrophysiological signals originating from the anterior
50 cingulate cortex. In line with similar response inhibition tasks, we found greater increases in
51 pre-response theta power when participants inhibited the response to shoot when under no
52 threat as compared to shooting. Most importantly, we showed that when preparing against
53 threat, theta power increase was greater for experts than novices, suggesting that differences
54 in performance between experts and novices are due to their greater orientation towards
55 threat. Additionally, shorter beta-rebounds suggest that experts were "ready for action"
56 sooner. More generally, we demonstrate that investigation of expert decision making should
57 incorporate naturalistic stimuli and an appropriate control group to enhance validity.

58 **Significance statement**

59 This study aims to unravel the complexities of how expertise affects neural processes during
60 uncertain scenarios by investigating police decision making. We present our variant on
61 shoot/don't shoot tasks which was co-developed with police instructors to allow graded levels
62 of force to elicit realistic responses. We show that experts exhibit superior performance in this
63 virtual reality-based task and that this is associated with greater modulation of frontal midline
64 theta activity prior to a decision. Understanding the intricacies of police decision making—
65 especially concerning the use of firearms—is vital to inform policy effectively. Further, the
66 naturalistic imaging methods employed here hold broader significance for neuroscientists
67 aiming to investigate real world behaviour.

68 **Introduction**

69 Authorised Firearms Officers (AFOs) of United Kingdom police forces can be authorised to
70 discharge a firearm within the bounds of domestic and international law (United Nations,
71 1990). While their intention is to apply stopping force, the result may be lethal. To inform policy,
72 deployment, and training aiming to minimise harm, it is imperative that effort is made to
73 understand the cognitive and underlying neurophysiological processes related to police
74 decision making and expertise (Rogers, 2003). We based our predictions on prior lab-based
75 research on neural signatures of action-related decision-making, (Walsh and Anderson, 2012;
76 Cavanagh and Frank, 2014; Eisma et al., 2021) expecting that basic aspects of neural
77 processing would generalise to realistic police-type decision making. In turn, we expected that
78 our findings within this crucial field of investigation would provide unique insight into how
79 specialised training in decision making may affect brain signatures more generally.

80 Recent reviews of research into police decision making have argued that they do not
81 consistently meet high methodological standards (Cox et al., 2014; Hope, 2016). For example,
82 novices, rather than police officers, are often studied (Correll et al., 2006; Pleskac et al., 2018;
83 Scott and Suss, 2019) and control groups are not always matched across demographics, such

84 as age (Nieuwenhuys et al., 2012a; Brisinda et al., 2015; Landman et al., 2016; Johnson et
85 al., 2018; Hamilton et al., 2019; Taylor, 2020), limiting the generalisability and validity of
86 findings, respectively. Despite this, studies of police decision making have benefited from the
87 use of naturalistic stimuli to promote ecological validity of results and to replicate the stress
88 induced by real-world firearms incidents that are not emulated in a standard computer-based
89 task (Cox et al., 2014; Sonkusare et al., 2019) and recent shoot/don't shoot (SDS) studies
90 have taken advantage of this method (Johnson et al., 2014; Taylor, 2020; Biggs and Pettijohn,
91 2022). Further, developments in virtual reality (VR) technology (Slater, 2018) provide
92 opportunity for even greater immersion and interactivity while still maintaining a high level of
93 experimental control (de la Rosa and Breidt, 2018).

94 In the current study, we created a SDS task presented using head mounted display (HMD)
95 based VR, enabling participation with negligible prior training specific to the experiment and
96 equipment. This allowed us to study expert AFO participants, as well as a control group of
97 age- and sex-matched non-police, novice participants, while they engaged with dynamic,
98 naturalistic scenarios in VR. Based on the expert advice of police instructors, we adapted the
99 standard SDS task (Correll et al., 2002) by using immersive VR to present scenarios with
100 graded threat levels, and realistic decisions that were split into two phases, a threat
101 assessment phase and a response phase. This ensured a closer link to real-world police
102 training and conflict situations.

103 To study components of electroencephalography (EEG) that are of interest to SDS decision
104 making we employed combined VR EEG methods. In particular, frontal midline theta (FM θ)
105 neural oscillations are related to action selection and initiation of executive control (Cavanagh
106 and Frank, 2014; Eisma et al., 2021) in decision making under uncertainty (Walsh and
107 Anderson, 2012). While the effects of expertise on SDS decision making are poorly
108 understood, we can draw on studies of similar response inhibition tasks to form hypotheses
109 about electrophysiological differences between SDS task conditions. For instance, expert
110 athletes in open skill sports, like tennis, perform better than novices in Go/No-Go tasks and
111 present with earlier and greater amplitude N200 event-related potential when inhibiting a
112 response (Di Russo et al., 2006; You et al., 2018), emphasising the importance of training and
113 expertise as contributing factors in decision making under uncertainty.

114 Our improved task, which was co-designed with police instructors, along with concurrent EEG,
115 allowed for unprecedented insight into the decision processes of police firearms experts during
116 assessment (Phase 1) and response (Phase 2) to threatening scenarios that significantly
117 extended beyond previous findings from earlier SDS paradigms. We expected group
118 differences in performance for both decision phases, with the expert group being faster at both
119 decision-making phases. Differences in response time between conditions in SDS tasks have
120 been consistently observed (Correll et al., 2002; Nieuwenhuys et al., 2012b), where the
121 decision to shoot is faster than the decision not to shoot. From our analysis of EEG neural
122 oscillations during decision making, we expected stronger FM θ for experts than matched
123 controls to emerge at the preparation phase. We also expected experts to elicit greater FM θ
124 than novices in the SDS phase. However, based on previous research, the Don't Shoot
125 condition of our SDS task should be associated with longer reaction times and greater FM θ
126 than the Shoot condition, an effect that could potentially be more pronounced in experts.
127 Finally, successful extraction of meaningful spectral signatures such as FM θ in a dynamic VR
128 scenario would provide a crucial proof-of-concept for future EEG-VR studies of expert decision
129 making. Such studies would increase realism and therefore the validity of neurocognitive
130 findings.

131 **Materials and Methods**

132 **Participants**

133 The experiment was completed by participants at three centres in the UK: Expert AFOs
134 completed the study at a police training centre; novice participants completed the study within
135 a comparable physical context at either Aston University or the University of Nottingham. All
136 participants gave their informed consent to participate in this study. The study was approved
137 by the Aston University Research Ethics Committee.

138 The Expert AFO group included 27 police officers with up-to-date training (College of Policing,
139 Police Firearms Training Curriculum). Their ages ranged from 27 to 53 ($M = 40.6$, $SD = 6.8$),
140 26 were male, two were left-handed (**Fig. 2B**). Their experience as police officers ranged from
141 five to 32 years ($M = 17.1$, $SD = 6.9$) and they had been AFOs for between one and 22 years
142 ($M = 10.6$, $SD = 7$).

143 We also recruited a Matched Control group of novice participants. Their ages ranged from 27
144 to 55 years ($M = 38.3$, $SD = 8.9$), 26 were male, 2 were left-handed. In addition, we collected
145 data from an Unmatched Novice group, with demographics (age and sex) representative of a
146 typical experiment cohort. This group was made up of 30 participants, but three were excluded
147 from analysis during data collection due to experimenter error. The 27 remaining participants'
148 ages ranged from 18 to 25 ($M = 20.4$, $SD = 2.6$), 12 were male, 3 were left-handed.

149 **Virtual reality setup**

150 *Head mounted display*

151 An Oculus Rift CV1 (Meta Platforms Inc., USA) HMD presented the experiment as a 3D virtual
152 environment using displays with a combined field of view of 110° and 1080x1200 resolution
153 per eye at a 90 Hz refresh rate. Participants responded using two Oculus Touch controllers
154 held in their hands. They wore an EEG cap underneath the HMD. A speaker in the room was
155 used for presenting audio, as the Oculus Rift CV1 headphones were not used, to reduce
156 electrical artefact.

157 The virtual human and environment were produced using Unreal Engine 4 (Epic Games Inc.,
158 USA). The environment comprised two walled courtyards separated by another wall with an
159 opening in the middle, which participants faced at the start of each trial (see **Fig. 1**). From their
160 perspective, the virtual human started each trial in the opposite courtyard, on the right,
161 concealed by the dividing wall. A single virtual human was used for all trials: a Caucasian
162 male, casually dressed and with a neutral expression.

163 *Action mapping*

164 Participants used virtual hands to engage with the task. Four buttons on the hand controller
165 allowed them to do this: a trigger for the index finger, a trigger for the middle finger, and two
166 buttons for the thumb. The middle finger trigger was used for grabbing firearms, the index
167 trigger for discharging firearms and the thumb buttons for pressing Safety and indicating
168 readiness to continue. Triggers could only be used on the dominant hand controller.

169 Two virtual holsters held both a Glock (a self-loading pistol/handgun used by AFOs) and a
170 Taser (a conducted energy device provided as a less lethal alternative use of force). The Glock
171 was placed close to the hip on the dominant side. The Taser was placed at the centre of the
172 chest. Firearms instructors advised that these are common placements for AFOs. Placement
173 was approximate as we used head tracking information only, and assumed the chest was just
174 below the head, and the hips further below and to the side. In order to grab a firearm using
175 the middle finger, participants first had to move their hand to the position of the desired virtual
176 holster. The onset of this movement was not recorded, *only the grabbing action itself*.

177 **Procedure**

178 *General procedure*

179 Regardless of expertise, participants were briefed in the same way and given the same
180 instructions. The HMD was set up and adjusted for comfort and clarity of display. Participants
181 then practiced the task under instruction until familiar. EEG was next applied, and the
182 participant was coached through minimising artefacts, by demonstrating the effect of talking
183 and moving muscles on the recording. They then completed the main experiment which was
184 made up of ten blocks of 20 trials, which took ~35 minutes.

185 *Task procedure*

186 Based on firearms instructor advice, each trial had two phases, risk assessment/preparation
187 (Phase 1) and SDS Decision (Phase 2) (see **Fig. 1**). The Weapon Presence condition
188 determined the stimulus presented at the Preparation stage, and virtual human Compliance
189 determined the stimulus presented at the Decision stage. Participants made one response per
190 stage in most instances. The only exception was when participants discharged their firearm
191 but missed the virtual human on the first (and possibly subsequent) attempt. Note, in these
192 instances, the trial was excluded from analysis. Participants were instructed that all responses
193 should be made as quickly and accurately as possible.

194 In Phase 1, the virtual human would walk from his starting position behind the right wall (from
195 the participant's perspective, completely obscured) to stand at the entrance in front of the
196 participant. In their hand they could hold a gun, a knife, or a drinks can. Previous research has
197 typically only compared a gun to a neutral condition (Correll et al., 2006; Nieuwenhuys et al.,
198 2012b). Our manipulation of three threat-levels and a choice of stopping force was again
199 based on the advice of firearms instructors to produce a realistic task in line with expected
200 behaviour from AFOs. The Weapon Presence condition (**Fig. 1**) determined which item was
201 held in the virtual human's hand and would appear as he came into view. Participants then
202 completed one of three preparation actions: equip Glock; equip Taser; or press Safety. Their
203 instructions told them that the correct preparation for each Weapon Presence condition was
204 to equip the Glock if the suspect held a Handgun, Taser if they held a Knife and press Safety
205 if they held a Drinks Can. Whichever action participants completed first was recorded as their
206 response: they could not change their mind during a trial. When Safety was pressed, a 'click'
207 sound was made and the firearms could no longer be equipped. When a firearm (either Glock
208 or Taser) was equipped, it could not be dropped or replaced with the other firearm. If equipped,
209 participants were instructed to aim the firearm at the centre of mass of the virtual human, in
210 preparation for the next stage.

211 The Decision stage began when the virtual human either Attacked or Surrendered, as
212 determined by the Compliance condition. The Surrender animation was always the same –
213 the virtual human would raise both hands while standing in place. The attack animation for the
214 Handgun involved the virtual human raising their hand to point it toward the participant. For
215 the Knife, the same arm animation was used but the virtual human also moved towards the
216 participant. All animations took one second to complete.

217 Participants could decide to either discharge their firearm or press the Safety button.
218 Whichever action they chose disabled the other. They were instructed to press Safety as soon
219 as they saw the virtual human surrendering. A click sound gave them feedback to let them
220 know the button had been pressed. Likewise, they were to shoot as soon as the virtual human
221 attacked. If they missed their shot, they were permitted to take another one. When the virtual

222 human was shot, his animation blended into a new animation and he fell to the ground. When
223 the Safety was pressed, the animation continued to its end. At the end of a trial the virtual
224 human disappeared, and any equipped firearms were automatically replaced in their holster.

225 Each of the possible combinations of Phase 1 and Phase 2 (Drinks Can, Surrender; Knife,
226 Attack; Knife, Surrender; Handgun, Attack; Handgun, Surrender) were repeated 40 times,
227 balanced across the ten blocks.

228 **EEG Analysis**

229 *On-line EEG Recording*

230 EEG data were recorded using an Eego sports system (ANT Neuro, Hengelo, Netherlands)
231 with 65-electrode (Ag/AgC) gel-based Waveguard caps which followed the 10-10 extension of
232 the International 10-20 system for electrode placement (Jasper, 1958). During recording,
233 electrodes were referenced to the CPz electrode and grounded at position AFz. All electrodes
234 were continuously sampled at 500 Hz and the median impedance of electrodes across all
235 recordings was 10.2 k Ω . Triggers sent via parallel port from the computer rendering the
236 experimental stimulus presented on the HMD were used to record stimulus presentation and
237 behavioural responses of participants directly into the EEG timeseries. The data were
238 organised into a Brain Imaging Data Structure (BIDS) compatible format (Niso et al., 2018).

239 *Pre-processing*

240 Two electrodes (M1, M2) were found to be corrupted by movement artefacts and were
241 removed before pre-processing. EEG data were then re-referenced to the common average
242 of all remaining electrodes. We applied Zapline (de Cheveigné, 2020) at 50 Hz (500ms
243 overlapping window, one component) to remove line noise, and 52.1 Hz (500ms component,
244 three components) to remove AC noise specific to the HMD (Weber et al., 2021). Next, data
245 were bandpass filtered (0.5-120 Hz passband, zero-phase, two-pass [forward and reverse],
246 Hamming-windowed, fourth-order digital Butterworth filter, -24dB/octave slope).

247 The continuous data were segmented into epochs defined from three seconds before to three
248 seconds after each trial where the participant responded correctly. Each epoch was visually
249 inspected for artefacts and if any were present, the whole epoch was excluded. An
250 independent components analysis (ICA) using the infomax algorithm (Bell and Sejnowski,
251 1995) was used to identify 61 independent components. Components identifiable as artefacts
252 (eye blink, eye movement, muscle activity, channel movement, electrocardiogram) were
253 removed (mean 5.5 components per dataset). The process of visual inspection and ICA was
254 iterative, as artefacts that could not be successfully removed with ICA were instead removed
255 at the trial level, and vice versa. For example, if when inspecting a component, it was apparent
256 that it was local to one trial (e.g. brief channel movement), we would remove the trial and re-
257 run the ICA, rather than removing the whole component. Only a single ICA decomposition was
258 performed per dataset. We did not attempt to use any automated artefact rejection techniques
259 as our sample size was small enough for visual inspection to be possible.

260 *Creating the forward model*

261 Individual head models were created from 3D scans taken of participants while wearing the
262 EEG cap. Following an established electrode digitisation pipeline (Homölle and Oostenveld,
263 2019), electrodes were localised by labelling the model and moving the electrode position
264 inwards by 8mm (electrode thickness). When permitted by participants' hair, head positions
265 on the forehead and back of the head were also measured. Electrodes and head positions

266 were then parsed as head digitisation coordinates to Brainstorm (Tadel et al., 2019). Within
267 Brainstorm, a template anatomy (ICBM152 2016c (Fonov et al., 2009)) which included a T1
268 structural MRI and boundary element model (BEM) of the scalp, skull and brain (Oostendorp
269 and van Oosterom, 1989), was warped to fit these landmarks using a non-linear transformation
270 (Ashburner and Friston, 1997).

271 The template and individual head models were used in Fieldtrip for further analysis. A leadfield
272 was created for the template using the 'dipoli' method in Fieldtrip with default conductivity
273 values (Gabriel et al., 1996). For each individual, a non-linear transformation between the
274 individual and template head model was calculated (Friston et al., 1995). The inverse of this
275 transformation was then applied to the template leadfield, and the output used as the individual
276 leadfield, allowing subsequent analysis to be conducted in a common space.

277 *Source localisation*

278 We estimated the source in the brain of each frequency band of interest to guide further
279 analysis at the virtual electrode level and to describe the data in the context of associated
280 brain regions. First, baseline (2000-1400ms pre-trial) and activity (250-850ms post-stimulus)
281 epochs were defined. The baseline period was selected as the time between trials in which
282 no condition-specific stimulus was presented on screen. Participants were at rest during this
283 period. The activity period was selected based on mean response times across conditions
284 (**Fig. 2**). The duration of the baseline and activity periods were equal to ensure equal
285 contribution to covariance. A duration of 600ms was chosen to allow a good estimation of
286 spectral power, even at low frequencies. Power and cross-spectral density within each
287 frequency band were calculated for baseline and activity epochs. These data were then
288 concatenated before calculating the inverse solution using exact low-resolution brain
289 electromagnetic tomography (eLORETA) (Pascual-Marqui et al., 1994). The common filter
290 was then applied to the baseline and activity epochs independently before contrasting the two
291 using decibel conversion. This contrast was then averaged across conditions and participants.
292 The coordinates of the maximum power of theta and the minimum power of alpha and beta
293 bands were used in the virtual electrode analysis (**Figs. 3C, 4, 5**).

294 *Virtual electrode calculation*

295 To estimate virtual electrode data at the peaks of activity for theta, alpha and beta, sensor
296 level data were segmented into epochs from -3000 to 3000ms around the stimulus in
297 conditions of interest. The time-locked average and associated covariance matrix were
298 calculated for each condition. These were used to estimate the inverse solution for the data
299 and the pre-calculated, individual forward models using a Linearly Constrained Minimum
300 Variance (LCMV) beamformer (Van Veen et al., 1997). The inverse solution was applied to
301 the individual epochs to provide virtual electrode data at the previously identified peaks for
302 each condition.

303 A time-frequency analysis of power was conducted from 1-32 Hz (1 Hz resolution) on the
304 virtual electrode data before averaging across trials within each participant and condition (see
305 **Fig. 3D,E**). This was done using the 'mtmconvol' (multi-taper method convolution) frequency
306 analysis in Fieldtrip. Despite the name, we used a single Hanning taper for all frequencies.
307 Power at each frequency was calculated within sliding time windows (20ms resolution). The
308 width of these time windows was set at four times the wavelength of the specified frequency.

309 Power values were baseline corrected from -2 to -1 seconds pre-trial using decibel (dB)
310 conversion and averaged across frequency, within the frequency bands of interest. Note that
311 baseline correct needed to be applied before statistical analysis of power because variations
312 in impedance between subjects and throughout recordings cause variation in observed power

313 across frequencies. Decibel conversion accounts for this by shifting the power value to a
314 relative measure that is consistent across subjects and over time. Further, in the case of
315 oscillatory power, it shifts the power distribution across time and channels to be normal and
316 within the assumptions of statistical test used.

317 **Experimental Design and Statistical Analysis**

318 We used non-parametric cluster-based permutation, as implemented in Fieldtrip (Maris and
319 Oostenveld, 2007; Oostenveld et al., 2010), when testing for within- and between-subject
320 comparisons. For within-subject comparisons, a two-tailed dependent samples t -test was used
321 as the permuted test statistic and for between-subject comparisons a two-tailed independent
322 samples t -test was used. In all cases, 10,000 permutations were taken with critical alpha-level
323 at .025 (after two-tailed correction), cluster alpha-level at .05 based on the 'maxsum' method
324 to correct for multiple comparisons within the test. Note, reported p -values are estimates
325 based on the distribution of the permuted cluster statistics. We have reported the temporal
326 bounds of clusters in brackets [start - end], but these should not be considered as explicit
327 boundaries. While non-parametric cluster-based permutation tests are suitable to test for
328 differences between data, they may not identify the full extent of a cluster.

329 **Code Accessibility**

330 EEG, behavioural data associated with this study and the code to prepare and analyse them
331 are available for download from the OpenNeuro data sharing platform (accession number
332 ds004877). They are prepared according to the EEG-BIDS data formatting standard.

333 **Results**

334 **Behavioural data**

335 *Matched control groups are essential when comparing expertise*

336 In addition to the Expert AFO and Matched Novice groups, we collected a third dataset of
337 Unmatched Novices (see *Materials and Methods*). For each group, we correlated age with
338 response time at Phase 1 and Phase 2 in the SDS task (**Fig. 2**). We found moderate positive
339 correlations between age and response time for Expert AFOs at Phase 1, $r(25) = 0.43$, $p =$
340 0.025 , and Phase 2, $r(25) = 0.51$, $p = 0.006$. Similar moderate correlations were found for the
341 Matched Novices group at Phase 2, $r(25) = 0.46$, $p = 0.016$, but only negligible correlations
342 were found at Phase 1, $r(25) = 0.33$, $p = 0.096$. Correlations for the Unmatched Novices were
343 also negligible at Phase 1, $r(25) = -.05$, $p = 0.82$, and Phase 2, $r(25) = -.09$, $p = 0.67$. These
344 findings are in line with studies of generalised response time and age which show a plateau
345 in early adulthood, followed by increasing positive correlation with age (Pierson and Montoye,
346 1958).

347 The Expert AFO and Matched Novice groups had only one female participant each, making
348 analysis of the effects of sex inappropriate. The Unmatched Novices group, however, had a
349 more balanced distribution of 12 males and 15 females, allowing for comparisons of the effects
350 of sex of mean response time using unpaired t -tests. At Phase 1, no significant difference was
351 found, $t(25) = 0.744$, $p = 0.46$. At Phase 2, males were found to be significantly faster than
352 females, $t(25) = -2.921$, $p = 0.007$. It is important to note that this effect is not applicable beyond
353 the Unmatched Novice group. We believe these findings highlight that between-subject
354 comparisons of expertise require careful control of participant age and, potentially, sex. This
355 is in addition to established variation in EEG oscillations across age and sex (Hoshi and
356 Shigihara, 2020). Therefore, although we included response time data from the Unmatched

357 Novice group in the subsequent behavioural analysis, we have focussed our analysis of EEG
358 on the Expert AFO and Matched Novice groups.

359 *Expert AFOs are quicker to respond at the Phase 1*

360 A 3 (between-subject, Expertise: Expert AFOs vs. Matched Novices vs. Unmatched Novices)
361 x 3 (within-subject, Weapon Presence: Can vs. Knife vs. Handgun) mixed factor analysis of
362 variance was used to test our hypothesis that response time would differ by expertise and
363 threat. Mauchly's test suggested that the assumption of sphericity was violated for the Weapon
364 Presence factor, so degrees of freedom were corrected for using Huynh-Feldt estimates of
365 sphericity ($\hat{\epsilon} = 0.78$). After sphericity corrections, a significant main effect of Weapon Presence
366 on response times at Phase 1 was observed, $F(1.57, 81.55) = 9.70$, $p < 0.001$, $\eta_{ges}^2 = 0.08$. A
367 significant main effect of Expertise was also found, $F(1, 52) = 5.07$, $p = 0.029$, $\eta_{ges}^2 = 0.05$.

368 No significant interaction between Expertise and Weapon Presence was found, $F(4, 156) =$
369 0.69 , $p = 0.6$, $\eta_{ges}^2 = 0.01$, and so the direction of the main effects was tested. Pairwise
370 comparisons (after Bonferroni correction) between Handgun and Knife were significant ($p <$
371 0.001 , $d = 0.49$), as were comparisons between Handgun and Drinks Can ($p = 0.004$, $d =$
372 0.47), but not between Knife and Drinks Can ($p = 1$, $d = 0.08$). This suggests that the main
373 effect of Weapon Presence was driven by faster response times in the Handgun condition
374 only. Similar pairwise comparisons were conducted for the main effect of Expertise. Expert
375 AFOs were significantly faster than Matched Novices ($p = 0.023$, $d = 0.61$). These results show
376 that the observed main effect of Group describes AFOs as significantly faster than Matched
377 Novices.

378 *Expertise resulted in faster decisions to shoot at the Phase 2*

379 A 3 (between-subject, Group: Expert AFOs vs. Matched Novices vs. Unmatched Novices) x 2
380 (within-subject, Weapon Presence: Knife vs. Handgun) x 2 (within-subject, Action: Surrender
381 vs. Attack) mixed factor analysis of variance was conducted. As expected, a main effect of
382 Action was found, $F(1, 78) = 315.81$, $p < 0.001$, $\eta_{ges}^2 = 0.59$. The effect size was large,
383 suggesting faster response times for firing in response to being attacked compared to pressing
384 safety in response to a surrender. No significant main effect was found either for Weapon type
385 (Knife vs Gun), $F(1, 78) = 0.31$, $p = 0.58$, $\eta_{ges}^2 < 0.01$, or for Group, $F(2, 78) = 1.37$, $p = 0.26$,
386 $\eta_{ges}^2 = 0.02$.

387 We had expected that Expert AFOs would be faster to respond in the Attack condition.
388 Surprisingly, neither a significant main effect for Group, $F(2, 78) = 1.37$, $p = 0.26$, $\eta_{ges}^2 = 0.02$
389 nor a significant interaction between Group and Action, $F(2, 78) = 2.55$, $p = 0.084$, $\eta_{ges}^2 = 0.02$,
390 were found. However, we conducted an additional pairwise comparison to test for the effect
391 of Group on the Attack condition of Action only as this was not directly tested by the main and
392 interaction effect analyses described. For this test, Levene's test for homogeneity of variance
393 approached significance ($F[2, 78] = 3.09$, $p = 0.051$) so we opted to use independent t -tests
394 without the assumption of equal variance for these pairwise comparisons. This contrast
395 showed that Expert AFOs' responses to shoot were significantly faster than Matched Novices',
396 $p = 0.001$, $d = 1.06$.

397 **EEG data**

398 *Separation and source localisation of oscillations*

399 Comparisons of EEG signals between groups and conditions were made by first identifying
400 and separating signals of interest from the total activity. An overview of this process can be
401 seen in **Fig. 3**. In brief, we estimated the cortical source of three frequency bands of interest,

402 theta, alpha and beta, independently (see *Materials and Methods – Source localisation*). The
403 coordinates of the maximum power of theta (dorsal anterior cingulate cortex [dACC], MNI [0,
404 0, 40]) and the minimum power of alpha (right angular gyrus, MNI [30 -60 20]) and beta (left
405 primary motor cortex, MNI [-20 -30 60]) versus baseline were then used to generate virtual
406 electrode signals.

407 *Theta response is greater in low- vs. high-threat conditions*

408 Comparisons between low- and high-threat conditions at Phase 1 and Phase 2 revealed
409 similar differences in theta power at a virtual electrode placed at the estimated peak of activity
410 in the dACC (**Fig. 4**). At Phase 1, we observed significantly greater pre-response theta when
411 equipping nothing versus equipping a firearm for both the Expert AFO [0.34s – 0.9s], $p <$
412 0.001, and Matched Novice groups [0.44s – 1.02s], $p <$ 0.001. At Phase 2, we observed
413 significantly greater pre-response theta activity when participants pressed safety versus
414 shooting their firearm for both the Expert AFOs [0.3s – 1.62s], $p <$ 0.001, and Matched Novices
415 [0.32s – 1.66s], $p <$ 0.001. In the Matched Novice group, we also observed an unexpectedly
416 early, significant positive cluster showing greater theta power in the Handgun condition [-0.02s
417 – 0.26s], $p =$ 0.039. Given the early timing and near threshold significance, this is likely a false
418 positive result.

419 *Expert AFOs show differences in theta when responding to graded levels of threat*

420 We also contrasted theta activity between trials where participants equipped a Taser versus
421 a Glock to see whether the measure was sensitive to the use of graded levels of force. For
422 the Expert AFO group, we found a similar pattern of activity to earlier contrasts which indicated
423 that lower threat level results in greater theta response: Expert AFOs had greater pre-
424 response theta activity when equipping a Taser versus a Glock [0.32s – 0.82s], $p =$ 0.018. For
425 the Matched Novice group, this contrast did not reveal any significant pre-response clusters.
426 However, we did observe a significant post-response cluster, showing greater theta power in
427 the Glock condition [1.1s – 1.54s], $p =$ 0.015.

428 *Expert AFOs have greater theta than Matched Novices when preparing a response to threat*

429 Between-subject comparisons between Expert AFOs and Matched Novices showed that the
430 experts had significantly greater theta activity when responding to threat than novices [0.1s –
431 0.72s], $p =$ 0.006. They also had significantly greater pre-response theta when responding to
432 no threat [0.1 – 0.7], $p =$ 0.005. See **Fig. 5A** for details. Although clusters with the same
433 direction of effect were found when comparing Expert AFOs' and Matched Novices' theta
434 activity at Phase 2 (**Fig. 5B**), they were not significant for the surrender [0.3s – 0.56s], $p =$
435 0.065, nor attack [0.38s – 0.48s], $p =$ 0.126, conditions. No significant pre-response
436 differences were found for alpha and beta frequency bands.

437 *Expert AFOs show reduced beta desynchronisation/faster beta rebound than Matched 438 Novices*

439 While our hypotheses were focussed on comparisons of pre-response theta, analysis of beta
440 band (13-32 Hz) power revealed interesting differences between Expert AFOs and Matched
441 Novices. In both conditions of Phase 1 (No Threat [1.06s – 1.44s], $p =$ 0.015; Threat [0.64s –
442 1.5s], $p =$ 0.006), experts showed an earlier beta rebound following their response, possibly
443 explained by a smaller initial beta desynchronisation pre-response. This effect was replicated
444 at Phase 2 in the Threat condition [0.42s – 1.24s], $p =$ 0.003.

445 **Discussion**

446 In the current study, expert police AFOs, an age- and sex-matched novice (non-police) group
447 and an unmatched novice group completed an SDS task in VR, in which they had to identify
448 and respond to possible threats in a series of two-phase scenarios. Analysis of response times
449 showed that AFOs consistently performed best, suggesting our task was sensitive to the
450 between-group expertise manipulation. Further, comparisons with the unmatched novice
451 sample included in our study at behavioural level underlined the requirement for matched age
452 distributions in studies comparing control groups with experts (**Fig. 2**). Subsequent analysis
453 of changes in pre-response oscillatory power at both phases of the SDS task revealed distinct
454 differences between the experts and their matched control group. Most notably, during the
455 preparation phase – when participants determined the appropriate response to varying levels
456 of threat – experts had greater estimated theta power in dACC, suggesting increased
457 orientation towards threatening stimuli.

458 Our research builds on other studies of police officer decision making that have used variations
459 of the SDS paradigm (Correll et al., 2002). However, research on EEG signals associated with
460 SDS decision making has so far been limited and the patterns of activity are not well
461 understood. Our analysis of EEG data allowed us to first identify the source of signals of
462 interest within the brain, and then to measure how the oscillatory activity modulated over time.
463 Generally, our analysis of theta, alpha and beta bands yielded the expected results across all
464 participant groups (**Figs. 4, 5**), conforming to demonstrated effects in a variety of traditional
465 experimental paradigms (Pfurtscheller and Lopes da Silva, 1999), as well as recent,
466 naturalistic paradigms (Walshe et al., 2023): when a stimulus is presented to participants and
467 they respond, theta power increases and alpha and beta power decreases.

468 Having confirmed this expected baseline pattern of activity across groups, we were able to
469 investigate how our experimental design affected these signals. When contrasting EEG-
470 derived virtual electrode signals time-locked to threatening and non-threatening stimuli, we
471 found that theta power attributed to the dACC was consistently higher across both phases of
472 the experiment and both groups when the stimulus was non-threatening versus threatening.
473 The estimated source of FM θ activity in the anterior cingulate cortex (ACC) is pertinent to its
474 role in decision making, as ACC is a well-connected hub of the brain (Cohen, 2011) and part
475 of the executive network (Petersen and Posner, 2012). The ACC is interconnected with the
476 basal ganglia structures of the reward circuit and the ventral striatum (Graybiel and Grafton,
477 2015; Jin and Costa, 2015; Saga et al., 2017). Through these pathways, faster response times
478 to threat observed in SDS tasks can be attributed to preferential, adaptive orientation towards
479 threatening stimuli (Lang et al., 1990; Öhman et al., 2001). Modulation of activity at ACC have
480 indeed been observed during SDS tasks and comparable response inhibition paradigms, such
481 as Go/No-Go tasks (Nieuwenhuis et al., 2003; Correll et al., 2006). Our task also shares a
482 common limitation with these tasks in that it is difficult to dissociate performance at the task
483 from motivation. It is possible that observed differences across our expertise manipulation
484 were in fact due to difference in motivation. However, the effect on behaviour and associated
485 neural activity is the same. It may be the case that increased motivation and focus are
486 inextricably linked to increasing expertise in these types of tasks.

487 Subsequent analysis of differences between groups addressed our main research question
488 about the effects of expertise on theta activity attributed to dACC. As expected, AFOs showed
489 greater dACC theta power when assessing the threat in scenarios. This may be related to a
490 more adaptive response to threat, whereby experts are able to reach a decision to respond or
491 inhibit a response quicker than novices. In contrast to our expectations, group differences
492 were not observed for dACC theta nor for alpha or beta frequencies during the second phase
493 of the SDS decision. This may indicate that the initial threat assessment and preparation were
494 crucial in the current scenarios and were significantly influenced by prior training and

495 expertise. Interestingly, however, after SDS responding, AFOs showed shorter beta-rebounds
496 compared to Matched Novices, which could indicate swifter recovery after executing an action
497 (Fig. 5B). In other words, AFOs might be “ready for action” after a shorter delay, which could
498 be another reflection of training and expertise.

499 It is important to note that these findings were obtained within a specific context: participants
500 were standing and engaging in a task in VR which required a considerable amount of
501 movement. This required adjustment to recording protocol and processing of EEG data to
502 minimise and suppress artefacts associated with movement (Klug and Gramann, 2021) and
503 HMD electronics (Weber et al., 2021). Stimulus presentation was naturalistic (Sonkusare et
504 al., 2019) and the timings that our analysis relied on were taken from a continuous
505 presentation of a virtual human in a scene. Further, participants’ interactions with VR affected
506 the stimuli in real-time, meaning that how participants chose to respond to the scenario and
507 actions were mapped to realistic movements and so varied between conditions. Therefore,
508 the fact our results are consistent with well-established findings from artificial, highly controlled
509 experiments such as the Go/No-Go task is promising for ongoing research using naturalistic
510 stimuli. Research using artificial stimuli benefits as well: replication of basic findings in studies
511 using naturalistic stimuli is an important demonstration of the validity of both (Rust and
512 Movshon, 2005). Note, our experimental design was necessarily repetitive and contrived to
513 benefit from a factorial design and sampling of underlying distributions in the data over time.
514 This could certainly have a negative effect on ecological validity. However, by allowing natural
515 behaviours within the bounds of the task we have shown that realistic behaviours can be
516 observed alongside electrophysiological signals.

517 Whereas advances in combined VR and neuroimaging (Roberts et al., 2019) and associated
518 analytical methods suggest that many new and interesting research questions can be
519 addressed using naturalistic imaging (De Sanctis et al., 2021), the feasibility of using these
520 methods to address a wide range of research questions varies. Part of the motivation for our
521 research was that, among “natural” expert behaviours, SDS decision making is particularly
522 amenable to EEG analysis because it occurs in a single, clearly defined moment: the pulling
523 of a trigger, or equipping a firearm. This was made clear to us after observing AFO training
524 and observing similarities between their methods and typical studies of human behaviour,
525 relating to response time and accuracy. Translating their training into a VR-EEG study enabled
526 us to increase realism to promote ecologically valid behaviours and EEG with minimal trade-
527 off for experimental control (Loomis et al., 1999; de la Rosa and Breidt, 2018). Additionally,
528 the use of VR allowed control participants to complete the scenarios without weapon training
529 and outside of specialised training facilities, so novices and experts could participate in the
530 same way. Overall, our study highlights the feasibility of VR-based tasks for investigating
531 police training and expertise more generally. These tasks can be effectively combined with
532 neuroimaging (Tromp et al., 2018), and so we call for a significant increase in ‘neuro-VR’
533 studies to address the impact of expertise and training on performance.

534 **Author contribution statement**

535 Conceptualization, K.K., M.J.B., S.B., N.A.A. Data curation, N.A.A. Formal Analysis, N.A.A.,
536 H.W., K.K. Funding acquisition, K.K., S.B., M.J.B. Investigation, N.A.A., C.L.K., H.W.
537 Methodology, N.A.A., K.K., R.A.N. Project administration, S.B., K.K. Software, N.A.A., C.L.K.
538 Supervision, K.K., M.J.B., R.A.N. Visualization, N.A.A. Writing – original draft, N.A.A., K.K.
539 Writing – review & editing, N.A.A., K.K., C.K., M.J.B., S.B., H.W, R.A.N.

540 **References**

- 541 Ashburner J, Friston KJ (1997) Multimodal Image Coregistration and Partitioning—A Unified
542 Framework. *NeuroImage* 6:209–217.
- 543 Bell AJ, Sejnowski TJ (1995) An Information-Maximization Approach to Blind Separation and
544 Blind Deconvolution. *Neural Computation* 7:1129–1159.
- 545 Biggs AT, Pettijohn KA (2022) The role of inhibitory control in shoot/don't-shoot decisions.
546 *Quarterly Journal of Experimental Psychology* 75:536–549.
- 547 Brisinda D, Venuti A, Cataldi C, Efremov K, Intorno E, Fenici R (2015) Real-time Imaging of
548 Stress-induced Cardiac Autonomic Adaptation During Realistic Force-on-force Police
549 Scenarios. *J Police Crim Psych* 30:71–86.
- 550 Cavanagh JF, Frank MJ (2014) Frontal theta as a mechanism for cognitive control. *Trends in*
551 *Cognitive Sciences* 18:414–421.
- 552 Cohen MX (2011) Error-related medial frontal theta activity predicts cingulate-related
553 structural connectivity. *NeuroImage* 55:1373–1383.
- 554 Correll J, Park B, Judd CM, Wittenbrink B (2002) The police officer's dilemma: Using
555 ethnicity to disambiguate potentially threatening individuals. *Journal of Personality*
556 *and Social Psychology* 83:1314–1329.
- 557 Correll J, Urland GR, Ito TA (2006) Event-related potentials and the decision to shoot: The
558 role of threat perception and cognitive control. *Journal of Experimental Social*
559 *Psychology* 42:120–128.
- 560 Cox WTL, Devine PG, Plant EA, Schwartz LL (2014) Toward a Comprehensive
561 Understanding of Officers' Shooting Decisions: No Simple Answers to This Complex
562 Problem. *Basic and Applied Social Psychology* 36:356–364.
- 563 de Cheveigné A (2020) ZapLine: A simple and effective method to remove power line
564 artifacts. *NeuroImage* 207:116356.
- 565 de la Rosa S, Breidt M (2018) Virtual reality: A new track in psychological research. *British*
566 *Journal of Psychology* 109:427–430.
- 567 De Sanctis P, Solis-Escalante T, Seeber M, Wagner J, Ferris DP, Gramann K (2021) Time
568 to move: Brain dynamics underlying natural action and cognition. *European Journal*
569 *of Neuroscience* 54:8075–8080.
- 570 Di Russo F, Taddei F, Apnile T, Spinelli D (2006) Neural correlates of fast stimulus
571 discrimination and response selection in top-level fencers. *Neuroscience Letters*
572 408:113–118.
- 573 Eisma J, Rawls E, Long S, Mach R, Lamm C (2021) Frontal midline theta differentiates
574 separate cognitive control strategies while still generalizing the need for cognitive
575 control. *Sci Rep* 11:14641.

- 576 Fonov V, Evans A, McKinstry R, Almli C, Collins D (2009) Unbiased nonlinear average age-
577 appropriate brain templates from birth to adulthood. *NeuroImage* 47:S102.
- 578 Friston KJ, Ashburner J, Frith CD, Poline J-B, Heather JD, Frackowiak RSJ (1995) Spatial
579 registration and normalization of images. *Human Brain Mapping* 3:165–189.
- 580 Gabriel S, Lau RW, Gabriel C (1996) The dielectric properties of biological tissues: II.
581 Measurements in the frequency range 10 Hz to 20 GHz. *Phys Med Biol* 41:2251.
- 582 Graybiel AM, Grafton ST (2015) The Striatum: Where Skills and Habits Meet. *Cold Spring
583 Harb Perspect Biol* 7:a021691.
- 584 Hamilton JA, Lambert G, Suss J, Biggs AT (2019) Can Cognitive Training Improve
585 Shoot/Don't-Shoot Performance? Evidence from Live Fire Exercises. *The American
586 Journal of Psychology* 132:179–194.
- 587 Homölle S, Oostenveld R (2019) Using a structured-light 3D scanner to improve EEG source
588 modeling with more accurate electrode positions. *Journal of Neuroscience Methods*
589 326:108378.
- 590 Hope L (2016) Evaluating the Effects of Stress and Fatigue on Police Officer Response and
591 Recall: A Challenge for Research, Training, Practice and Policy. *Journal of Applied
592 Research in Memory and Cognition* 5:239–245.
- 593 Hoshi H, Shigihara Y (2020) Age- and gender-specific characteristics of the resting-state
594 brain activity: a magnetoencephalography study. *Aging (Albany NY)* 12:21613–
595 21637.
- 596 Jasper HH (1958) The Ten Twenty Electrode System of the International Federation.
597 *Electroenceph clin Neurophysiol* 10:371–375.
- 598 Jin X, Costa RM (2015) Shaping action sequences in basal ganglia circuits. *Current Opinion
599 in Neurobiology* 33:188–196.
- 600 Johnson DJ, Cesario J, Pleskac TJ (2018) How prior information and police experience
601 impact decisions to shoot. *Journal of Personality and Social Psychology* 115:601–
602 623.
- 603 Johnson RR, Stone BT, Miranda CM, Vila B, James L, James SM, Rubio RF, Berka C
604 (2014) Identifying psychophysiological indices of expert vs. novice performance in
605 deadly force judgment and decision making. *Front Hum Neurosci* 8:512.
- 606 Klug M, Gramann K (2021) Identifying key factors for improving ICA-based decomposition of
607 EEG data in mobile and stationary experiments. *European Journal of Neuroscience*
608 54:8406–8420.
- 609 Landman A, Nieuwenhuys A, Oudejans RRD (2016) The impact of personality traits and
610 professional experience on police officers' shooting performance under pressure.
611 *Ergonomics* 59:950–961.
- 612 Lang PJ, Bradley MM, Cuthbert BN (1990) Emotion, attention, and the startle reflex.
613 *Psychological Review* 97:377–395.

- 614 Loomis JM, Blascovich JJ, Beall AC (1999) Immersive virtual environment technology as a
615 basic research tool in psychology. *Behavior Research Methods, Instruments, &*
616 *Computers* 31:557–564.
- 617 Maris E, Oostenveld R (2007) Nonparametric statistical testing of EEG- and MEG-data.
618 *Journal of Neuroscience Methods* 164:177–190.
- 619 Nieuwenhuis S, Yeung N, van den Wildenberg W, Ridderinkhof KR (2003)
620 Electrophysiological correlates of anterior cingulate function in a go/no-go task:
621 Effects of response conflict and trial type frequency. *Cognitive, Affective, &*
622 *Behavioral Neuroscience* 3:17–26.
- 623 Nieuwenhuys A, Cañal-Bruland R, Oudejans RRD (2012a) Effects of Threat on Police
624 Officers' Shooting Behavior: Anxiety, Action Specificity, and Affective Influences on
625 Perception. *Applied Cognitive Psychology* 26:608–615.
- 626 Nieuwenhuys A, Savelsbergh GJP, Oudejans RRD (2012b) Shoot or don't shoot? Why
627 police officers are more inclined to shoot when they are anxious. *Emotion* 12:827–
628 833.
- 629 Niso G, Gorgolewski KJ, Bock E, Brooks TL, Flandin G, Gramfort A, Henson RN, Jas M,
630 Litvak V, Moreau JT, Oostenveld R, Schoffelen J-M, Tadel F, Wexler J, Baillet S
631 (2018) MEG-BIDS, the brain imaging data structure extended to
632 magnetoencephalography. *Sci Data* 5:180110.
- 633 Öhman A, Lundqvist D, Esteves F (2001) The face in the crowd revisited: A threat
634 advantage with schematic stimuli. *Journal of Personality and Social Psychology*
635 80:381–396.
- 636 Oostendorp TF, van Oosterom A (1989) Source parameter estimation in inhomogeneous
637 volume conductors of arbitrary shape. *IEEE Transactions on Biomedical Engineering*
638 36:382–391.
- 639 Oostenveld R, Fries P, Maris E, Schoffelen J-M (2010) FieldTrip: Open Source Software for
640 Advanced Analysis of MEG, EEG, and Invasive Electrophysiological Data.
641 *Computational Intelligence and Neuroscience* 2011:e156869.
- 642 Pascual-Marqui RD, Michel CM, Lehmann D (1994) Low resolution electromagnetic
643 tomography: a new method for localizing electrical activity in the brain. *International*
644 *Journal of Psychophysiology* 18:49–65.
- 645 Petersen SE, Posner MI (2012) The Attention System of the Human Brain: 20 Years After.
646 *Annu Rev Neurosci* 35:73–89.
- 647 Pfurtscheller G, Lopes da Silva FH (1999) Event-related EEG/MEG synchronization and
648 desynchronization: basic principles. *Clinical Neurophysiology* 110:1842–1857.
- 649 Pierson WR, Montoye HJ (1958) Movement Time, Reaction Time and Age. *Journal of*
650 *Gerontology* 13:418–421.
- 651 Pleskac TJ, Cesario J, Johnson DJ (2018) How race affects evidence accumulation during
652 the decision to shoot. *Psychon Bull Rev* 25:1301–1330.

- 653 Roberts G, Holmes N, Alexander N, Boto E, Leggett J, Hill RM, Shah V, Rea M, Vaughan R,
654 Maguire EA, Kessler K, Beebe S, Fromhold M, Barnes GR, Bowtell R, Brookes MJ
655 (2019) Towards OPM-MEG in a virtual reality environment. *NeuroImage* 199:408–
656 417.
- 657 Rogers MD (2003) Police Force! An Examination of the Use of Force, Firearms and Less-
658 Lethal Weapons by British Police. *The Police Journal* 76:189–203.
- 659 Rust NC, Movshon JA (2005) In praise of artifice. *Nat Neurosci* 8:1647–1650.
- 660 Saga Y, Richard A, Sgambato-Faure V, Hoshi E, Tobler PN, Tremblay L (2017) Ventral
661 Pallidum Encodes Contextual Information and Controls Aversive Behaviors. *Cerebral*
662 *Cortex* 27:2528–2543.
- 663 Scott D, Suss J (2019) Perceptual Anticipation in a Shoot/Don't Shoot Task. *Proceedings of*
664 *the Human Factors and Ergonomics Society Annual Meeting* 63:1358–1362.
- 665 Slater M (2018) Immersion and the illusion of presence in virtual reality. *British Journal of*
666 *Psychology* 109:431–433.
- 667 Sonkusare S, Breakspear M, Guo C (2019) Naturalistic Stimuli in Neuroscience: Critically
668 Acclaimed. *Trends in Cognitive Sciences* 23:699–714.
- 669 Tadel F, Bock E, Niso G, Mosher JC, Cousineau M, Pantazis D, Leahy RM, Baillet S (2019)
670 MEG/EEG Group Analysis With Brainstorm. *Frontiers in Neuroscience* 13.
- 671 Taylor PL (2020) Dispatch Priming and the Police Decision to Use Deadly Force. *Police*
672 *Quarterly* 23:311–332.
- 673 Tromp J, Peeters D, Meyer AS, Hagoort P (2018) The combined use of virtual reality and
674 EEG to study language processing in naturalistic environments. *Behav Res* 50:862–
675 869.
- 676 United Nations (1990) Basic Principles on the Use of Force and Firearms by Law
677 Enforcement Officials. In: *Eighth United Nations Congress on the Prevention of*
678 *Crime and the Treatment of Offenders, Revision 1.*, pp 110–116. Havana: United
679 Nations.
- 680 Van Veen BD, Van Drongelen W, Yuchtman M, Suzuki A (1997) Localization of brain
681 electrical activity via linearly constrained minimum variance spatial filtering. *IEEE*
682 *Transactions on Biomedical Engineering* 44:867–880.
- 683 Walsh MM, Anderson JR (2012) Learning from experience: Event-related potential
684 correlates of reward processing, neural adaptation, and behavioral choice.
685 *Neuroscience & Biobehavioral Reviews* 36:1870–1884.
- 686 Walshe EA, Roberts TPL, Ward McIntosh C, Winston FK, Romer D, Gaetz W (2023) An
687 event-based magnetoencephalography study of simulated driving: Establishing a
688 novel paradigm to probe the dynamic interplay of executive and motor function.
689 *Human Brain Mapping* 44:2109–2121.

690 Weber D, Hertweck S, Alwanni H, Fiederer LDJ, Wang X, Unruh F, Fischbach M, Latoschik
691 ME, Ball T (2021) A Structured Approach to Test the Signal Quality of
692 Electroencephalography Measurements During Use of Head-Mounted Displays for
693 Virtual Reality Applications. *Frontiers in Neuroscience* 15.

694 You Y, Ma Y, Ji Z, Meng F, Li A, Zhang C (2018) Unconscious response inhibition
695 differences between table tennis athletes and non-athletes. *PeerJ* 6:e5548.

696 **Figure Legends**

697 **Figure 1.** Examples of stimuli from two scenarios. Between the pre-trial baseline period and
698 Phase 1, the virtual human walked from behind the wall, into view. Two examples of threat at
699 Phase 1 can be seen (Handgun and Knife), as well as the two possible outcomes in Phase 2
700 (Surrender and Attack). Note, these examples are snapshots from a continuous stimulus
701 presentation to an HMD, so the precise presentation varied continuously with participant
702 movement and the display technology presented it as a high-resolution 3D scene.

703 **Figure 2.** Summary of response time analysis at the two decision points. Upper panel (**A**)
704 shows the results from Phase 1 of the task, where participants decided to equip either Nothing,
705 a Taser or a Glock. Participants were faster to respond to threat (Knife/Handgun) than no
706 threat (Drinks Can) and Expert AFO response times were faster than both novice groups at
707 the preparation decision. Lower panel (**B**) shows the results from the SDS decision in Phase
708 2. Again, participants were faster to respond to threat (Attack) versus no threat (Surrender),
709 and Expert AFOs were faster to respond to threat than both novice groups at the SDS decision
710 stage. Additional descriptions of the effects of age can be seen on the right of each panel,
711 along with the age distributions of each group shown with box-and-whisker plots of the inter-
712 quartile range. Note, error bars on bar charts show the standard error of the mean, black bars
713 highlight significant differences with asterisked references to the level of significance.

714 **Figure 3.** Overview of EEG data preparation and source localisation. **A** and **B** show the sensor
715 level time-frequency data for Expert AFO and Matched Novice participants averaged across
716 trials where a weapon was present, and the virtual human attacked. For the time-frequency
717 representation figures (top), the average of the central nine electrodes was taken (FC1, FC2,
718 Cz, CP1, CP2, FCz, C1, C2, CPz) and baseline corrected against data from -2s to -1s using
719 decibel (dB) conversion. In these figures, data are time-locked to the onset of both stimuli,
720 which were always 4s apart: Weapon Presence (0s, Phase 1) and Compliance (4s, Phase 2).
721 On-scalp topographies of frequencies of interest from 250-750ms are shown. **C** illustrates the
722 source estimation for the theta, alpha and beta bands using eLORETA. White crosshairs show
723 the peak activity for each band. **D** and **E** show time-frequency data for virtual electrodes placed
724 at the peaks estimated in **C**, but for each group separately. Note, all colour axes are formed
725 of two linear sub-scales: from zero to the maximum value and from zero to the minimum value,
726 to highlight the topography of each signal.

727 **Figure 4.** Within-subject comparisons of theta (3-7 Hz) power at a virtual electrode positioned
728 at the positive peak in theta activity averaged across all groups (MNI: [0 0 40], Dorsal Anterior
729 Cingulate Cortex). The right and left panels show that when inhibiting a response (Equip
730 Nothing, Phase 1, or press Safety, Phase 2) both groups of participants exhibit greater dACC
731 theta power versus responding to threat (Equip Firearm, phase 1, and Shoot Firearm, phase
732 2). The central panel shows that only Expert AFOs demonstrate greater theta power when
733 equipping a Taser versus a Glock in Phase 1. Vertical dashed lines represent stimulus onset
734 (black) and average response times (orange or purple). Black horizontal lines indicate the

735 presence and duration of significant clusters. Shaded areas around lines show the standard
736 error of the mean.

737 **Figure 5.** Comparisons of theta, alpha and beta activity between Expert AFO and Matched
738 Novice groups within critical decision points. In each case, power has been calculated from a
739 virtual electrode placed at the positive (theta) or negative (alpha, beta) peak of oscillatory
740 power in the brain. **A** shows comparisons from the Preparation Stage (Phase 1) when there
741 was no threat and when there was a threat. The main finding was that Expert AFOs showed
742 significantly higher pre-response theta power than the Matched Novices in both conditions. A
743 shorter beta-rebound was also observed for AFOs compared to Matched Novices after
744 response in both conditions. **B** shows comparisons from the SDS decision (Phase 2). No
745 significant pre-response differences were found. A shorter beta-rebound was again observed
746 for AFOs compared to Matched Novices after response, but only in the Threat + Attack
747 condition. Dashed vertical lines represent stimulus onset (black) and mean group response
748 times (red or blue). Black horizontal lines indicate the presence and duration of significant
749 clusters. Shaded areas around lines show the standard error of the mean.

eNeuro Accepted Manuscript

Pre-trial baseline period



Phase 1 - Handgun



Phase 2 - Surrender



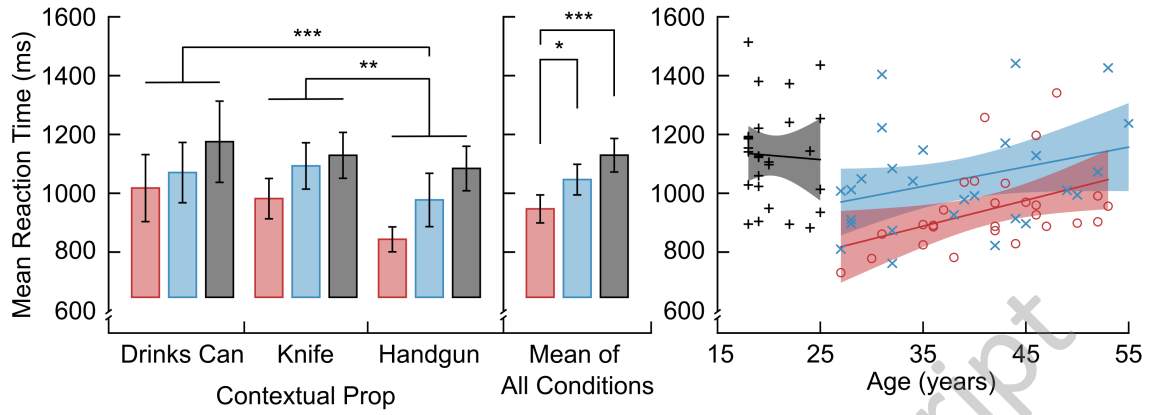
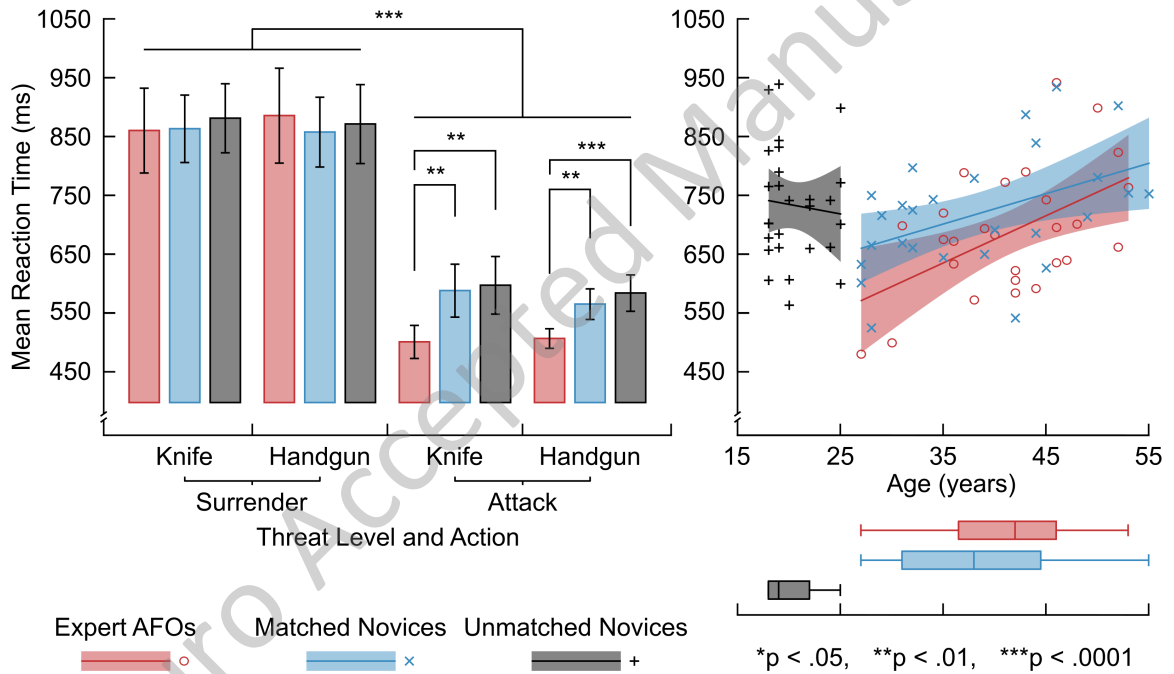
Phase 1 - Knife

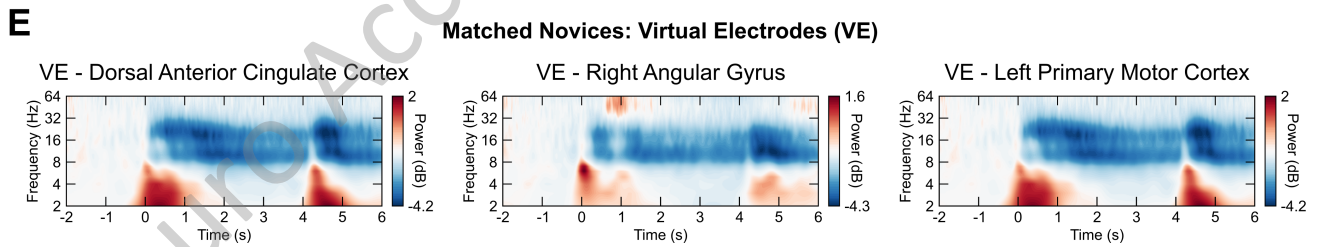
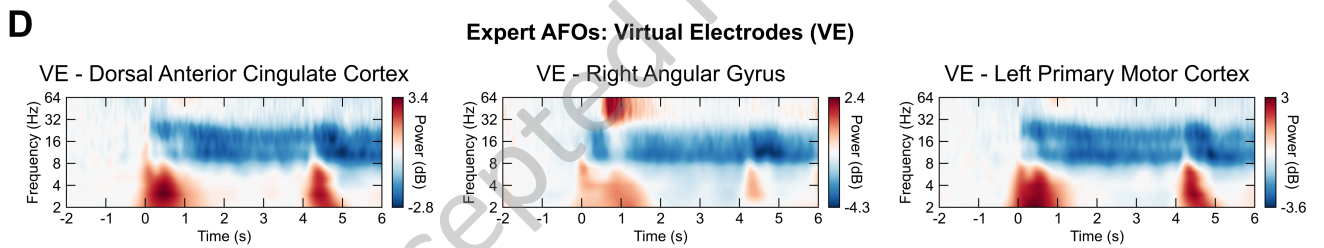
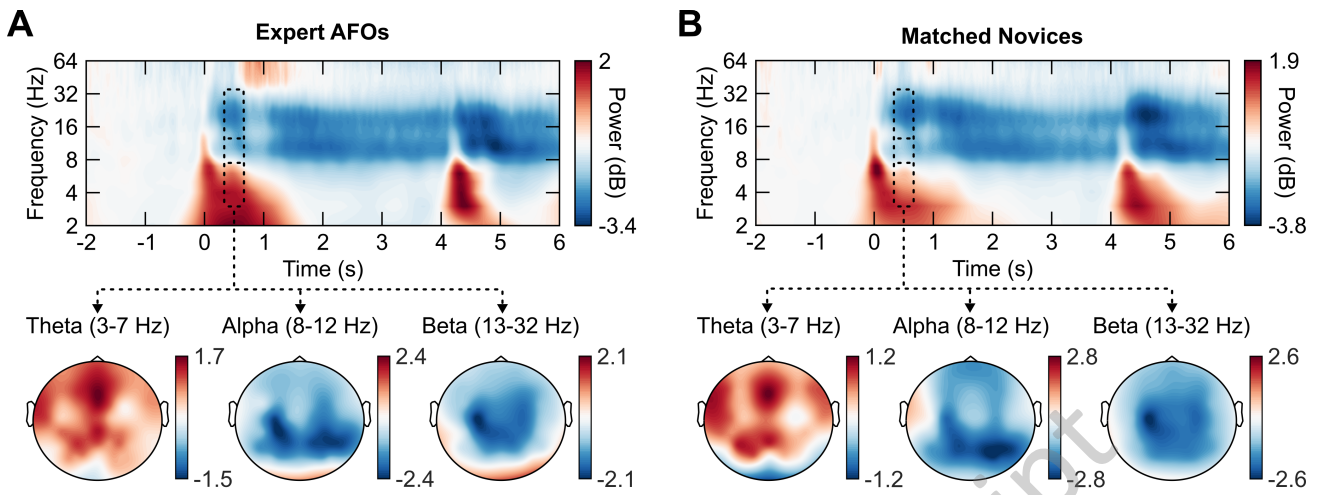


Phase 2 - Attack



eNeuro Accepted

A**Phase 1: Equip Nothing/Taser/Glock****B****Phase 2: Shoot/Don't Shoot Taser/Glock**



Within-Subject Theta (3-7 Hz) Analysis

